Published in final edited form as:
J Am Coll Cardiol. 2013 March 12; 61(10): 1041–1051. doi:10.1016/j.jacc.2012.10.054.

Histopathologic Characteristics of Atherosclerotic Coronary Disease and Implications of the Findings for the Invasive and Noninvasive Detection of Vulnerable Plaques

Jagat Narula, MD, PhD[*], **Masataka Nakano, MD, PhD**[†], **Renu Virmani, MD**[†], **Frank D. Kolodgie, PhD**[†], **Rita Petersen, MS**[‡], **Robert Newcomb, PhD**[‡], **Shaista Malik, MD, PhD**[‡], **Valentin Fuster, MD, PhD**[*,§], and **Aloke V. Finn, MD**[‖]
New York, New York; Gaithersburg, Maryland; Irvine, California; Madrid, Spain; and Atlanta, Georgia

Abstract

Objectives—The goal of this study was to identify histomorphologic characteristics of atherosclerotic plaques and to determine the amenability of some of these components to be used as markers for invasive and noninvasive imaging.

Background—Rupture of the atherosclerotic plaques is responsible for the majority of acute coronary events, and the culprit lesions demonstrate distinct histopathologic features. It has been tacitly believed that plaque rupture (PR) is associated with angiographically minimally occlusive lesions.

Methods—We obtained 295 coronary atherosclerotic plaques, including stable (fibroatheroma [FA]; n = 105), vulnerable (thin-cap fibroatheroma [TCFA]; n = 88), and disrupted plaques (plaque rupture [PR]; n = 102) from the hearts of 181 men and 32 women who had died suddenly. The hierarchical importance of fibrous cap thickness, percent luminal stenosis, macrophage area, necrotic core area, and calcified plaque area was evaluated by using recursive partitioning analysis. Because clinical assessment of fibrous cap thickness is not possible by noninvasive imaging, it was excluded from the second set of partitioning analysis.

Results—Thickness of the fibrous cap emerged as the best discriminator of plaque type; the cap thickness measured <55 μm in ruptured plaques, and all FA were associated with >84-μm cap thickness. Although the majority of TCFA were found in the 54- to 84-μm thickness group, those with <54-μm thickness were more likely to show <74% luminal stenosis (area under the curve: FA, 1.0; TCFA, 0.89; PR, 0.90). After exclusion of cap thickness, analysis of the plaque characteristics revealed macrophage infiltration and necrotic core to be the 2 best discriminators of plaque types (area under the curve: FA, 0.82; TCFA, 0.58; PR, 0.72). More than 75% cross-section area stenosis was seen in 70% of PR and 40% of TCFA; only 5% PR and 10% TCFA were <50% narrowed.

Reprint requests and correspondence: Dr. Jagat Narula, Zena and Michael A. Weiner Cardiovascular Institute, Mount Sinai School of Medicine, One Gustave L. Levy Place, Box 1030, New York, New York 10029. narula@mountsinai.org.
[*]Mount Sinai School of Medicine, New York, New York;
[†]Cardiovascular Pathology Institute, Gaithersburg, Maryland;
[‡]University of California, Irvine, School of Medicine, Irvine, California;
[§]Centro Nacional de Investigaciones Cardiovasculares Carlos III, Madrid, Spain;
[‖]Emory University School of Medicine, Atlanta, Georgia.
The first 2 authors contributed equally to this work.

The authors have reported that they have no relationships relevant to the contents of this paper to disclose.

Conclusions—This postmortem study defines histomorphologic characteristics of vulnerable plaques, which may help develop imaging strategies for identification of such plaques in patients at a high risk of sustaining acute coronary events.

Keywords

acute coronary syndrome; coronary artery disease; high-risk plaque; positive remodeling

Acute myocardial infarction or sudden coronary death may occur as the first manifestation of coronary disease in a large proportion of otherwise asymptomatic subjects, and the importance of the identification of subjects at a very high risk of developing such events cannot be overemphasized.

An acute coronary event has been traditionally considered as an unavoidable manifestation of coronary atherosclerosis (1). However, it is becoming increasingly clear that although the victims of such events often have subclinical disease, they usually harbor standard risk factors (2). Framingham risk score has been routinely applied for stratification of asymptomatic subjects into low-, intermediate-, and high-risk categories for the development of acute coronary events (3). Almost 10% of adults in the United States and Western Europe belong to the high-risk category with an event rate expected to be >2% per year (3,4). As recommended in an elegant editorial, such individuals, in addition to intense global risk factor reduction, may be better served by further identification of vulnerable plaques in those who are at very high risk (i.e., >15% acute coronary events per year) (1). With the prevention of such events as the primary goal, the onus is on the imagers to identify these “accidents waiting to happen” (2).

Postmortem studies have established plaque rupture (PR) to be the cause of up to 75% of episodes of acute coronary syndromes. The disrupted plaques in proximal coronary arteries usually have a large necrotic core with a thin overlying fibrous cap (1,5–10); these lesions are substantially inflamed and have little calcification. It is believed that they do not cause critical narrowing of the coronary lumen because of outward (expansive or positive) remodeling of the arterial segment (11–16). It has been proposed that the lesions with similar histomorphologic characteristics but intact fibrous caps are vulnerable to rupture. For the current study, we obtained a large number of coronary atherosclerotic plaques from the victims of sudden cardiac death to determine the importance of various pathological characteristics (including fibrous cap thickness, percent luminal stenosis, plaque area, necrotic core area, macrophage area, and calcification) in the stable plaques (fibroatheroma [FA]), vulnerable plaques (thin-cap fibroatheroma [TCFA]), and PR. We proposed that the hierarchical importance of various histomorphologic characteristics would allow us to develop diagnostic strategies for invasive and noninvasive imaging of vulnerable plaques.

Methods

We evaluated 295 coronary atherosclerotic plaques dissected from the hearts of 181 male and 32 female victims of sudden cardiac death sent to the Cardiovascular Pathology Institute (Gaithersburg, Maryland) for diagnostic consultation from the medical examiner’s office. All specimens were carefully perfusion-fixed in 10% buffered formalin for the accurate measurement of the luminal stenoses. Epicardial arteries were then removed from the heart, radiographed, and processed for histopathologic examination (6,16). The left main coronary artery, as well as the proximal and middle segments of the 3 arteries, were examined up to the acute marginal branch of the right coronary artery, second diagonal branch of the left anterior descending, and second obtuse marginal branch of the left circumflex artery. Distal segments and all branches were excluded from the analysis. The dissected segments of

coronary arteries were serially sectioned at 3- to 4-mm intervals and processed for histological examination. Severely calcified sections recognized under radiograph were treated with ethylenediamine-tetraacetic acid (only when decalcification was considered necessary). All sections were stained with hematoxylin and eosin, as well as with Movat pentachrome. Atherosclerotic plaques were classified as follows: Vulnerable plaque (TCFA) was defined as the lesion with thin fibrous cap with infiltration of macrophages (6,17) and ruptured plaque (PR) by the presence of acute luminal thrombus with connection to lipid-rich necrotic core through the disruption of thin fibrous cap (Figs. 1 and 2). Stable plaque (FA) was described as a plaque with well-matured necrotic core covered by thick fibrous cap rich in smooth muscle cell or healed plaque rupture (i.e., interruption of the fibrous cap with newly formed thick intimal coverage) (18). TCFA adjacent to PR and FA adjacent to TCFA were excluded so that a longitudinally distributed plaque may not be repetitively included.

Quantitative morphometry was performed by using computerized planimetry (IPLab, Scanalytics, Inc., Rockville, Maryland). Sections were magnified and digitized, and the luminal, internal elastic lamina (IEL), and external elastic lamina (EEL) areas were measured. Plaque area was defined as the difference between IEL and luminal area measurements. Percent luminal stenosis was calculated as the plaque area/IEL area × 100. This value is the pathologically defined luminal stenosis and may not accurately represent an angiographic decrease in lumen area. Fibrous cap thickness was measured at the thinnest part of the fibrous cap or its remnant at the site of the ruptured plaque. In addition, areas occupied by the necrotic core and calcified matrix were assessed in each segment as previously described (17,19). Immunohistochemical stains were performed for CD68 (KP1 clone; Dako Corporation, Carpinteria, California), and the positive area by using color threshold was measured as macrophage infiltration.

Statistical analyses

We evaluated the relationship between the pathological characteristics and the 3 defined plaque types according to both univariate and multivariable methods. Based on the initial evaluation of distributions, descriptive statistics included mean ± SD, as well as medians and ranges of the pathological features, including fibrous cap thickness (TCAP), EEL and IEL, plaque and lumen areas, percent lumen stenosis, necrotic core size, percent necrotic core, macrophage count per high-power field, percent macrophage area, and total and percent calcification area. Preliminary univariate analyses consisted of applying nonparametric methods to assess which features initially seemed to provide value in a final multivariate model. We used the Kruskal-Wallis test for evaluating differences between plaque types for each of the features under consideration. In addition, each feature was evaluated by applying Cunick's test of trend (20), a nonparametric method based on the assumption of an ordinality of the plaque categories including FA, TCFA, and PR. Plaque type was also compared with the traditionally used 3 categories (<50%, >50% to <75%, and >75%) of cross-sectional luminal stenosis and tested with a chi-square test for independence. Our primary goal was to apply a multivariate method, which, rather than assume and test any a priori model, would descriptively explore the structure of the data with respect to the dominance of individual plaque characteristics and combinations of features that may jointly influence plaque rupture. Recursive partitioning analysis (RPA), also known as classification tree analysis, is well suited for this purpose. The method is free of distributional and linearity assumptions, incorporates interactions, and allows for the re-entry of candidate variables in distinguishing subgroups (21).

RPA was first employed by using TCAP, percent luminal stenosis and luminal diameter, macrophage area, necrotic core area, and calcified plaque area as candidate predictor

variables. Because clinical assessment of TCAP is not amenable to noninvasive imaging, we excluded TCAP in the second set of RPA.

Each resulting classification tree was evaluated by using a sample reuse method (training-test subsets) with a 5-fold cross validation, which resulted in a cross-validated R^2. An overall R^2 based on the portion of the log-likelihood attributed to the model was also included. Each variable's contribution to the total resulting chi-square statistic was also examined. Finally, a receiver-operating characteristic curve was generated to quantify the accuracy of the model's overall classification ability. RPA was also performed separately for 2 subsets of the data based on 50% to 75% and >75% categories of stenosis, with and without inclusion of TCAP. Less than 50% stenosis was excluded because of the small sample size (n = 19). All analyses were performed by using JMP version 8.0 (SAS Institute Inc., Cary, North Carolina), and details of model validation and evaluation can be found in JMP 8 Statistics and Graphics Guide (22).

Results

Of the 295 coronary atherosclerotic plaques, lesions were pathologically classified as FA (n= 105), TCFA (n = 88), and PR (n = 102) (Figs. 1 and 2). Preliminary evaluation of plaque features indicated skewed distributions for continuous variables (Table 1), with all tests for normality being rejected at $p < 0.001$. Kruskal-Wallis tests showed statistically significant differences according to plaque type (at $p < 0.01$ level) for all features, with the exception of total and percent calcification. Trend test indicated statistically significant trends in the levels of each characteristic ($p < 0.001$), with the exception of percent lumen stenosis and both measures of calcification. Distributions of categories of stenosis within plaque type varied, as shown by the chi-square test ($p < 0.0004$) (Table 2).

Analysis of plaque characteristics

Analysis of 102 PR found >75% cross-section area stenosis in 70% of instances and 50% to 75% stenosis in 25% of the ruptured plaques; only 5% of the PR had <50% cross-section area stenosis (Figs. 2 and 3). Conversely, 40% of the 88 TCFA showed >75% cross-sectional area stenosis, and 50% of TCFA showed stenosis of 50% to 75%; 10% of the TCFA had <50% cross-section area stenosis. The difference in distribution of the extent of stenosis in TCFA and PR (obtained from different deceased subjects) may suggest that the plaques that rupture are substantially narrowed at the time of the acute event, and it is rare to find disrupted but nonstenotic plaques (Fig. 3).

RPA allowed us to identify the morphological characteristics in hierarchical importance that segregated PR, TCFA, and PR (Figs. 4 and 5). For the multivariable RPA model, which included all cases and all candidate variables, TCAP emerged as the dominant plaque characteristic in its ability to discriminate between 3 plaque types. TCAP thickness was always ≥84 μm in FA (Fig. 4) (Table 2); the plaques that were <84 μm at their thinnest diameter included almost all TCFA and PR. Further partitioning revealed that the fibrous caps associated with PR measured <54 μm at the site of rupture. Therefore, the plaques covered by ≥84-μm TCAP were stable, and PR demonstrated fibrous cap attenuation to <54 μm. Although the majority of TCFA were found in the 54- to 84-μm thickness group, a subset of TCFA showed <54-μm TCAP. By the next step of RPA, those TCFA plaques that demonstrated <54-μm cap thickness (and had not yet disrupted) were more likely to show <74% cross-section area stenosis. This finding allows us to support the contention that vulnerable plaques will need to encroach farther on the lumen and demonstrate critical fibrous cap thinning before an actual event. This signifies the importance of a combination of TCAP and luminal stenosis as the best measure for identifying the natural history of plaques.

RPA after exclusion of TCAP

Because TCAP is only amenable to invasive imaging methods and thus would not be clinically practical for screening asymptomatic subjects, we repeated the RPA excluding TCAP from analysis (Fig. 4, Table 2). The segregation of the 3 types of plaques was not as clear as it was when TCAP was included. Of the remaining plaque characteristics, plaque inflammation allowed separation of PR and TCFA from FA. The discriminatory level of inflammation was >0.21 mm^2 macrophage area per high-power microscopic field area. Although most of FA demonstrated lack of substantial inflammation, a small proportion of PR and TCFA segregated with the group of less than the discriminatory level of inflammation. Less inflamed PR and TCFA could be separated from FA by the simultaneous presence of a necrotic core area >3.5 mm^2. A minority of TCFA remained in the less inflamed and small necrotic core group with FA, and plaque inflammation once again allowed further separation of FA in the third step of RPA. It seems logical to propose that inflamed plaques and large necrotic cores are 2 key features of plaque vulnerability when TCAP is not available.

Discussion

The current study suggests that TCAP, whenever available, offers the best discriminator of a vulnerable plaque (Table 2). The <54-μm cap thickness in PR is similar to the thickness reported clinically by using optical coherence tomography interrogation of culprit lesions in patients presenting with acute coronary events (23,24). This investigation also reveals that the fibrous caps are thicker than 84 μm in plaques bearing the pathological features of stable plaques. Most TCFA fall in the 54- to 84-μm range. Some TCFA, which demonstrate <54-μm TCAP, are usually associated with <74% luminal stenosis. It seems logical to propose that when intravascular imaging information is available, the lesions with <85-μm thick cap (rounding the figure to the nearest multiple of 5) and >75% cross-sectional luminal area stenosis should alert the clinicians. This pathological study confirms the results of the recent prospective natural history study of plaque vulnerability PROSPECT (Providing Regional Observations to Study Predictors of Events in the Coronary Tree), wherein the greater plaque burden (>70%), smaller luminal diameter (<4 mm^2), and intravascular ultrasound–based TCFA were associated with adverse outcomes during a 3.4-year follow-up (25). The plaque burden (area) did not emerge as a significant determinant of plaque vulnerability in our study, and it seems logical to propose that precise information about TCAP with the degree of luminal stenosis may overshadow the importance of plaque burden. It also seems logical to believe that a thin cap with luminally obstructive lesion would be associated with large plaque burden predominantly arising from inflamed and necrotic core–rich morphology. Further investigation, similar to PROSPECT, is warranted to clinically confirm the importance of TCAP in luminally stenotic lesions; optical coherence tomography with a resolution of <10 μm may allow better definition of TCAP (23,24,26).

The luminal stenosis loses its importance as the predictor of a vulnerable plaque when TCAP is not available as a candidate variable, and morphological characterization of plaque becomes important to demonstrate the magnitude of plaque inflammation and the necrotic cores. Strategies for the noninvasive assessment of these 2 plaque features will therefore need to be developed. Necrotic cores have been identified as low-attenuation plaque areas (<30 HU) on coronary CT angiography imaging, which are frequently associated with expansive remodeling (>110%) of the affected coronary segments (27–29). CT angiography is also able to demonstrate the extent of luminal stenosis with reasonable accuracy (30). Positively remodeled low-attenuation plaques as identified by using CT angiography were associated with a 22.5% adverse event rate over a 2-year follow-up period, compared with <0.5% in the absence of these plaque characteristics (29). The low-attenuation plaque (and

volume) was larger and the extent of remodeling greater in the plaques that subsequently developed an acute event (Table 3). Furthermore, the greater the remodeling index and the larger the necrotic core size, the earlier the acute coronary event occurred in follow-up. The positively remodeled plaques on CT angiography showing the necrotic core area of <0.5 mm^2 did not result in acute coronary syndrome. Unlike the feasibility of necrotic core size assessment, there is as yet no available clinical method to accurately assess degree of plaque inflammation. Although increased circulating levels of inflammatory biomarkers (e.g., high-sensitivity C-reactive protein) portend unfavorable outcomes, no postmortem study has yet reported its relationship with the extent of macrophage inflammation in the culprit atherosclerotic lesions (31,32). It has recently been proposed that the extent of macrophage-based inflammation in plaques can be identified by combined CT angiography and positron emission tomography imaging employing fluorine-18–labeled 2-fluorodeoxyglucose (FDG) (33–35).

FDG-based positron emission tomography in carotid arteries has been correlated with the extent of macrophage infiltration in carotid endarterectomy specimens and is more often associated with symptomatic disease (36–38). Although anecdotal reports of FDG uptake in coronary plaques were available (39,40), a recent study has reported FDG uptake in culprit lesions in patients presenting with acute coronary events and a lack thereof in lesions in patients presenting with stable coronary syndromes (33). Such an imaging strategy would need considerable improvement because it currently requires restricting myocardial FDG uptake for sufficient contrast resolution by feeding a high-fat diet to the patients (33,34).

The current study also offers intriguing insights into plaque biology. Whereas two-thirds of the PR demonstrated >75% cross-section area narrowing (Fig. 3), the majority of TCFA showed 50% to 75% luminal narrowing. We therefore extrapolate that the TCFA may need to expand or grow bigger before they rupture. Alternatively, it can be explained that among many of the potentially vulnerable plaques, only the few that are severely stenotic eventually rupture. However, the angiography report in which the information about angiographic stenosis was available at the time of an acute coronary event and also 1 year earlier (41) supports the progression of plaques before they rupture; the culprit lesion had substantially grown and the extent of luminal compromise increased significantly during the period of observation. The PROSPECT study also prospectively confirmed that the mean angiographic diameter stenosis of the 106 lesions subsequently responsible for major adverse cardiovascular events was 32 ± 21% at baseline and 65 ± 16% at 3.4-year follow-up ($p < 0.001$) (25). The amenability of luminally occlusive lesions for plaque rupture is not contradictory to the belief that the fateful plaques responsible for acute coronary events are more likely to be mildly obstructive (11–13). This assumption of the association of <50% luminal obstruction with culprit lesions has been based primarily on reports in which the previous coronary angiograms happened to be available for a review. As discussed earlier, the availability of serial angiograms confirms the interval progression in the luminal stenosis before the occurrence of a coronary event (25,41). In addition, noninvasive stress tests using radionuclide and ultrasound imaging have revealed significant prognostic value of the inducible ischemia for predicting major adverse cardiac events (42–45), alluding to the prognostic significance of flow-limiting coronary lesions. More recent studies using CT angiography and magnetic resonance imaging have produced similar results for all ages and both sexes (46–50).

Relatively rapid increase in plaque volume reportedly results from intraplaque hemorrhage in acute carotid events (51) and is almost always seen before the event (52). A similar role for plaque hemorrhage has been proposed for acute coronary events (53,54). However, although erythrocyte extravasation is observed to a variable extent in coronary plaques (29,31) and is known to correlate with the magnitude of necrotic core size, intraplaque

hemorrhages are less common than carotid vasculature. Another possible mechanism could involve the plaque attaining the Glagovian limit of positive remodeling; it is plausible that failing to further expand outward, the plaque encroaches on the lumen (16). Most importantly, the repeated plaque rupture and healing cycles are very common in coronary arteries and contribute substantially to plaque growth; the greater the number of previous ruptures, the larger the plaque volume (55). It is logical to presume that a thinner cap of significantly stenotic lesions would be more amenable to mechanical rupture and an acute event in response to hemodynamic perturbations. Conversely, the less stenotic TCFA may hypothetically be more amenable to rupture-healing cycles.

Study limitations

First, there was a lack of clinical information in these patients and firm data regarding whether the vessel was an infarct-related artery. The study specimens were sent to us from the medical examiner's office, wherein not much clinical information is usually available. Therefore, although these plaques were carefully analyzed, there was no information on the real culprit lesion in many of these patients. Second, although this study included plaque area as an important histological parameter, information about the positive remodeling was lacking; this would have required pathological characterization of the entire vascular length. Third, all parameters were acquired in a cross-section and not from the longitudinal study of the plaque. Therefore, the necrotic core size was defined wherever the minimum luminal diameter was seen and the thinnest TCAP was measured in the same section. Unlike the pathological studies, the intravascular imaging technology and coronary CT angiography reports have the advantage of describing the disease both at the cross-sectional level (in terms of area calculation) and by the analysis of entire plaque longitudinally (for the volume calculation). Fourth, the role of intraplaque hemorrhage was not independently addressed, and the area of hemorrhage was included within the necrotic core area. Fifth, the use of autopsy data may not be representative of plaque morphology in patients who have coronary artery disease and survive. Finally, this study only addressed the plaque rupture and its precursor as the substrate for acute coronary syndrome and does not include the culprit plaques characterized by endothelial erosion responsible for up to one-third of acute coronary events (6,56).

Conclusions

This postmortem study defines histomorphologic characteristics of vulnerable plaques, which may help development of invasive and noninvasive imaging strategies for identification of such lesions in patients at a high risk of sustaining acute coronary events. Although this study offers measurable indicators of plaque vulnerability, better tools for preselection of high-risk patients will need to be identified because the available noninvasive imaging procedures inflict nonnegligible levels of radiation burden. Conversely, invasive characterization of high-risk patients, although not feasible on a large-scale basis, seems to have distinct advantages in terms of being able to measure more accurately more powerful classifiers of risk such as TCAP and may find a place in decision making during coronary interventions.

Abbreviations and Acronyms

CT	computed tomography
EEL	external elastic lamina
FA	fibroatheroma

FDG	fluorine-18-labeled 2-fluorodeoxyglucose
IEL	internal elastic lamina
PR	plaque rupture
RPA	recursive partitioning analysis
TCAP	fibrous cap thickness
TCFA	thin-cap fibroatheroma

References

1. Braunwald E. Epilogue: what do clinicians expect from imagers? J Am Coll Cardiol. 2006; 47(Suppl c):C101–3. [PubMed: 16631504]
2. Braunwald E. Noninvasive detection of vulnerable coronary plaques: locking the barn door before the horse is stolen. J Am Coll Cardiol. 2009; 54:58–9. [PubMed: 19555841]
3. Wilson PW, D'Agostino RB, Levy D, et al. Prediction of coronary heart disease using risk factor categories. Circulation. 1998; 97:1837– 47. [PubMed: 9603539]
4. Wood D, De Backer G, Faergeman O, et al. Prevention of coronary heart disease in clinical practice: recommendations of the Second Joint Task Force of European and Other Societies on Coronary Prevention. Eur Heart J. 1998; 19:1434–503. [PubMed: 9820987]
5. Davies MJ. The composition of coronary-artery plaques. N Engl J Med. 1997; 336:1312–4. [PubMed: 9113937]
6. Burke AP, Farb A, Malcom GT, Liang YH, Smialek J, Virmani R. Coronary risk factors and plaque morphology in men with coronary disease who died suddenly. N Engl J Med. 1997; 336:1276–82. [PubMed: 9113930]
7. Narula J, Strauss HW. The popcorn plaques. Nat Med. 2007; 13:532–4. [PubMed: 17479093]
8. Fuster V, Badimon L, Badimon JJ, Chesebro JH. The pathogenesis of coronary artery disease and the acute coronary syndromes (1). N Engl J Med. 1992; 326:242–50. [PubMed: 1727977]
9. Fuster V, Badimon JJ, Chesebro JH. The pathogenesis of coronary artery disease and the acute coronary syndromes (2). N Engl J Med. 1992; 326:310–8. [PubMed: 1728735]
10. Narula J, Garg P, Achenbach S, Motoyama S, Virmani R, Strauss HW. Arithmetic of vulnerable plaques for noninvasive imaging. Nat Rev Cardiol. 2008; 5 (Suppl 2):S2–10.
11. Ambrose JA, Winters SL, Arora RR, et al. Angiographic evolution of coronary artery morphology in unstable angina. J Am Coll Cardiol. 1986; 7:472–8. [PubMed: 3950227]
12. Ambrose JA, Winters SL, Stern A, et al. Angiographic morphology and the pathogenesis of unstable angina pectoris. J Am Coll Cardiol. 1985; 5:609–16. [PubMed: 3973257]
13. Falk E, Shah PK, Fuster V. Coronary plaque disruption. Circulation. 1995; 92:657–71. [PubMed: 7634481]
14. Schoenhagen P, Ziada KM, Kapadia SR, et al. Extent and direction of arterial remodeling in stable versus unstable coronary syndromes. Circulation. 2000; 101:598–603. [PubMed: 10673250]
15. Yamagishi M, Terashima M, Awano K, et al. Morphology of vulnerable coronary plaque. J Am Coll Cardiol. 2000; 35:106–11. [PubMed: 10636267]
16. Glagov S, Weisenberg E, Zarins CK, Stankunavicius R, Kolettis GJ. Compensatory enlargement of human atherosclerotic coronary arteries. N Engl J Med. 1987; 316:1371–5. [PubMed: 3574413]
17. Virmani R, Kolodgie FD, Burke AP, Farb A, Schwartz SM. Lessons from sudden coronary death: a comprehensive morphological classification scheme for atherosclerotic lesions. Arterioscler Thromb Vasc Biol. 2000; 20:1262–75. [PubMed: 10807742]
18. Mann J, Davies MJ. Mechanisms of progression in native coronary artery disease: role of healed plaque disruption. Heart. 1999; 82:265–8. [PubMed: 10455072]
19. Burke AP, Kolodgie FD, Farb A, Weber D, Virmani R. Morphological predictors of arterial remodeling in coronary atherosclerosis. Circulation. 2002; 105:297–303. [PubMed: 11804983]

20. Cuzick JA. Wilcoxon-type test for trend. Stat Med. 1985; 4:87–90. [PubMed: 3992076]
21. Zhang, H.; Singer, B. Recursive Partitioning in Health Sciences. New York, NY: Springer-Verlag; 1999.
22. SAS Institute Inc. JMP 8 Statistics and Graphics Guide. 2. Cary, NC: SAS Institute, Inc; 2009. p. 809-32.
23. Yonetsu T, Kakuta T, Lee T, et al. In vivo critical fibrous cap thickness for rupture-prone coronary plaques assessed by optical coherence tomography. Eur Heart J. 2011; 32:1251–9. [PubMed: 21273202]
24. Jang IK, Tearney GJ, MacNeill B, et al. In vivo characterization of coronary atherosclerotic plaque by use of optical coherence tomography. Circulation. 2005; 111:1551–5. [PubMed: 15781733]
25. Stone GW, Maehara A, Lansky AJ, et al. for the PROSPECT Investigators. A prospective natural-history study of coronary atherosclerosis. N Engl J Med. 2011; 364:226–35. [PubMed: 21247313]
26. Hattori K, Ozaki Y, Ismail TF, et al. Impact of statin therapy on plaque characteristics as assessed by serial optical coherence tomography, grayscale and integrated-backscatter intravascular ultrasound. J Am Coll Cardiol Img. 2012; 5:169–77.
27. Motoyama S, Kondo T, Anno H, et al. Atherosclerotic plaque characterization by 0. 5-mm-slice multislice computed tomographic imaging. Circ J. 2007; 71:363–6. [PubMed: 17322636]
28. Motoyama S, Kondo T, Anno H, et al. Multi-slice compute tomographic characteristics of coronary lesions in acute coronary syndromes. J Am Coll Cardiol. 2007; 50:319–26. [PubMed: 17659199]
29. Motoyama S, Sarai M, Harigaya H, et al. Computed tomographic angiography characteristics of atherosclerotic plaques subsequently resulting in acute coronary syndrome. J Am Coll Cardiol. 2009; 54:49–57. [PubMed: 19555840]
30. Budoff MJ, Dowe D, Jollis JG, et al. Diagnostic performance of 64-multidetector row coronary computed tomographic angiography for evaluation of coronary artery stenosis in individuals without known coronary artery disease: results from the prospective multicenter ACCURACY (Assessment by Coronary Computed Tomographic Angiography of Individuals Undergoing Invasive Coronary Angiography) trial. J Am Coll Cardiol. 2008; 52:1724–32. [PubMed: 19007693]
31. Ridker PM. Clinical application of C-reactive protein for cardiovascular disease detection and prevention. Circulation. 2003; 107:363–9. [PubMed: 12551853]
32. Burke AP, Tracy RP, Kolodgie F, et al. Elevated C-reactive protein values and atherosclerosis in sudden coronary death: association with different pathologies. Circulation. 2002; 105:2019–23. [PubMed: 11980679]
33. Rogers IS, Nasir K, Figueroa AL, et al. Feasibility of FDG imaging of the coronary arteries: comparison between acute coronary syndrome and stable angina. J Am Coll Cardiol Img. 2010; 3:388–97.
34. Narula J, Chandrashekhar Y. Molecular imaging of coronary inflammation: overcoming hurdles one at a time. J Am Coll Cardiol Img. 2010; 3:448–50.
35. Tawakol A, Finn AV. Imaging inflammatory changes in atherosclerosis: multimodal imaging hitting stride. J Am Coll Cardiol Img. 2011; 4:1119–22.
36. Tawakol A, Migrino RQ, Bashian GG, et al. In vivo ^{18}F-fluorodeoxyglucose positron emission tomography imaging provides a noninvasive measure of carotid plaque inflammation in patients. J Am Coll Cardiol. 2006; 48:1818–24. [PubMed: 17084256]
37. Davies JR, Rudd JH, Fryer TD, et al. Identification of culprit lesions after transient ischemic attack by combined ^{18}F-fluorodeoxyglucose positron-emission tomography and high-resolution magnetic resonance imaging. Stroke. 2005; 36:2642–7. [PubMed: 16282536]
38. Tahara N, Imaizumi T, Virmani R, Narula J. Clinical feasibility of molecular imaging of plaque inflammation in atherosclerosis. J Nucl Med. 2009; 50:331–4. [PubMed: 19223412]
39. Dunphy MP, Freiman A, Larson SM, Strauss HW. Association of vascular 18F-FDG uptake with vascular calcification. J Nucl Med. 2005; 46:1278–84. [PubMed: 16085583]
40. Alexanderson E, Slomka P, Cheng V, et al. Fusion of positron emission tomography and coronary computed tomographic angiography identifies fluorine ^{18}F-fluorodeoxyglucose uptake in the left main coronary artery soft plaque. J Nucl Cardiol. 2008; 15:841–3. [PubMed: 18984461]

41. Glaser R, Selzer F, Faxon DP, et al. Clinical progression of incidental, asymptomatic lesions discovered during culprit vessel coronary intervention. Circulation. 2005; 111:143–9. [PubMed: 15623544]
42. Iskandrian AS, Heo J, Mostel E. The role of radionuclide cardiac imaging in coronary artery bypass surgery. Am Heart J. 1987; 113:163–70. [PubMed: 3492133]
43. Rahimtoola SH, Dilsizian V, Kramer CM, Marwick TH, Vanover-schelde JL. Chronic ischemic left ventricular dysfunction: from patho-physiology to imaging and its integration into clinical practice. J Am Coll Cardiol Img. 2008; 1:536–55.
44. Bjork Ingul C, Rozis E, Slordahl SA, Marwick TH. Incremental value of strain rate imaging to wall motion analysis for prediction of outcome in patients undergoing dobutamine stress echocardiography. Circulation. 2007; 115:1252–9. [PubMed: 17325245]
45. Schoenhagen P, Hachamovitch R, Achenbach S. Coronary CT angiography and comparative effectiveness research prognostic value of atherosclerotic disease burden in appropriately indicated clinical examinations. J Am Coll Cardiol Img. 2011; 4:492–5.
46. Pundziute G, Schuijf JD, Jukema JW, et al. Prognostic value of multislice computed tomography coronary angiography in patients with known or suspected coronary artery disease. J Am Coll Cardiol. 2007; 49:62–70. [PubMed: 17207724]
47. Shaw LJ, Narula J. Cardiovascular imaging quality: more than a pretty picture! J Am Coll Cardiol Img. 2008; 1:266–9.
48. Coelho-Filho OR, Seabra LF, Mongeon FP. Stress myocardial perfusion imaging by CMR provides strong prognostic value to cardiac events regardless of patient's sex. J Am Coll Cardiol Img. 2011; 4:850– 61.
49. Shaw LJ, Narula J. Beyond the glass ceiling—achieving gender equity in risk stratification for cardiovascular imaging. J Am Coll Cardiol Img. 2011; 4:924–5.
50. Shaw LJ, Narula J. Coronary CT angiography: an established, not emerging, basis of diagnosis and risk stratification. J Am Coll Cardiol Img. 2011; 4:565–6.
51. Takaya N, Yuan C, Chu B, et al. Presence of intraplaque hemorrhage stimulates progression of carotid atherosclerotic plaques: a high-resolution magnetic resonance imaging study. Circulation. 2005; 111:2768–75. [PubMed: 15911695]
52. Takaya N, Yuan C, Chu B, et al. Association between carotid plaque characteristics and subsequent ischemic cerebrovascular events: a prospective assessment with MRI—initial results. Stroke. 2006; 37:818–23. [PubMed: 16469957]
53. Kolodgie FD, Gold HK, Burke AP, et al. Intraplaque hemorrhage and progression of coronary atheroma. N Engl J Med. 2003; 349:2316–25. [PubMed: 14668457]
54. Virmani R, Kolodgie FD, Burke AP, Finn AV, Tulenko TN, Narula J. Atherosclerotic plaque progression and vulnerability to rupture: angiogenesis as a source of intraplaque hemorrhage. Arterioscler Thromb Vasc Biol. 2005; 25:2054–61. [PubMed: 16037567]
55. Burke AP, Kolodgie F, Farb A, et al. Healed plaque rupture and sudden cardiac death: evidence that subclinical rupture has a role in plaque progression. Circulation. 2001; 103:934–40. [PubMed: 11181466]
56. Ozaki Y, Okumura M, Ismail TF, et al. Coronary CT angiographic characteristics of culprit lesions in acute coronary syndromes not related to plaque rupture as defined by optical coherence tomography and angioscopy. Eur Heart J. 2011; 32:2814–23. [PubMed: 21719455]

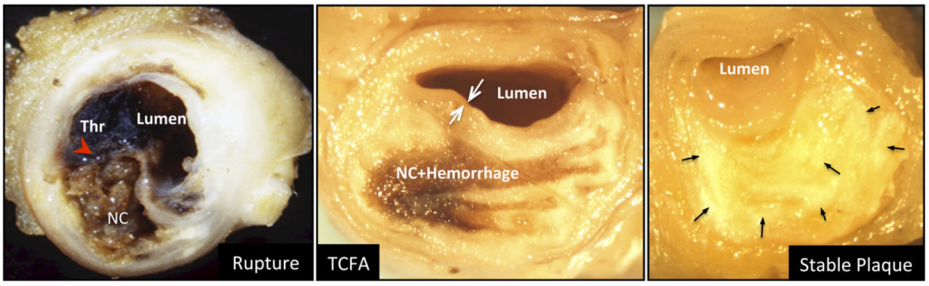

Figure 1. Gross Morphology of Human Coronary Artery With Disrupted, Vulnerable (TCFA), and Stable (FA) Plaques

(Left) Plaque rupture (PR), showing disruption of fibrous cap at the shoulder region of the plaque **(red arrowhead)** and thrombus (Thr) superimposed. **(Middle)** An example of thin-cap fibroatheroma (TCFA). A large hemorrhagic necrotic core (NC) is observed within the plaque. **White arrows** are pointing to the thinnest portion of the fibrous cap. **(Right)** Stable plaque. The plaque mainly consists of fibrous tissue with calcification **(black arrows)**. FA = fibroatheroma.

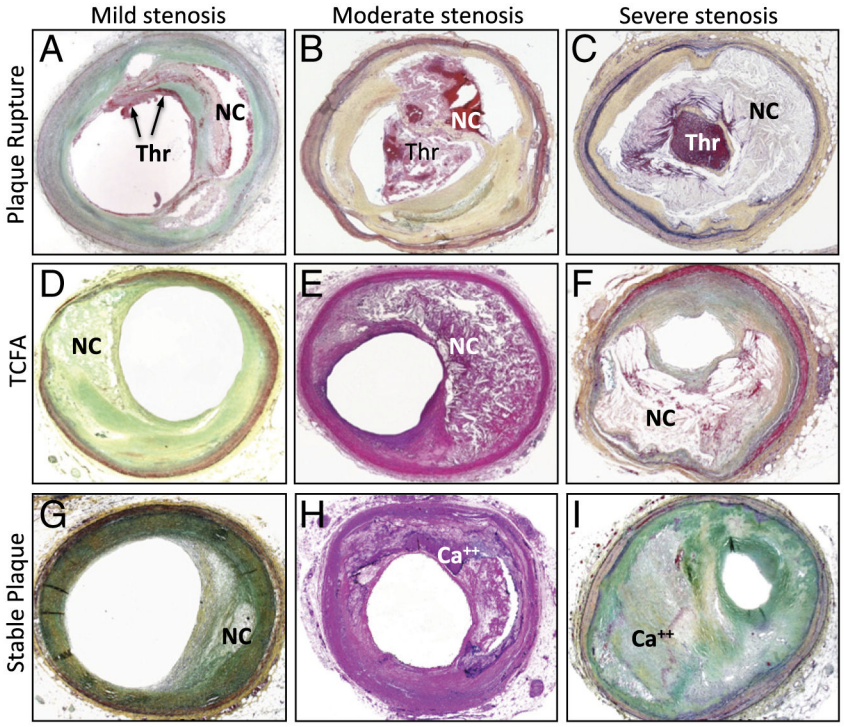

Figure 2. Photomicrographic Cross-Section of Human Coronary PR, TCFA, and FA With Varying Degree of Luminal Stenosis

(A to C) Plaque rupture with mild, moderate, and severe luminal stenosis, respectively. Nonocclusive Thr is observed in the microphotograph A whereas occlusive Thr is occupying the lumen in the image **B and C. (D to F)** TCFA with mild, moderate, and severe luminal stenosis, respectively. NC is covered by a thin fibrous cap, and Thr is not present in the lumen. **(G to I)** Stable plaque or FA with mild, moderate, and severe luminal stenosis, respectively. The size of necrotic core is relatively small when present, and calcification (Ca^{++}) is frequently seen. Abbreviations as in Figure 1.

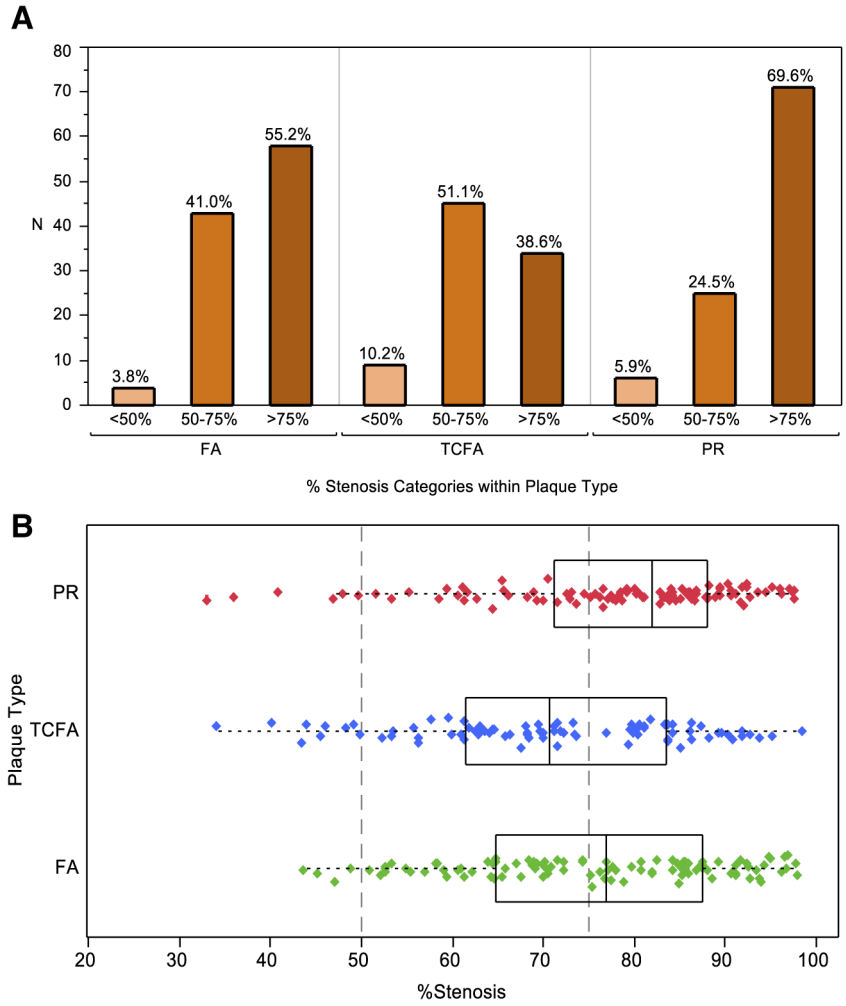

Figure 3. Luminal Obstruction in FA, TCFA, and PR

(A) Bar graph and **(B)** boxplot show >50% cross-sectional vascular area stenosis in a majority of PR and TCFA. The distribution indicates that TCFA may further enlarge before plaque rupture. Boxplot shows numerical data through the lower quartile, median, and upper quartile, and the whiskers represent the sample minimum and sample maximum observations. Abbreviations as in Figure 1.

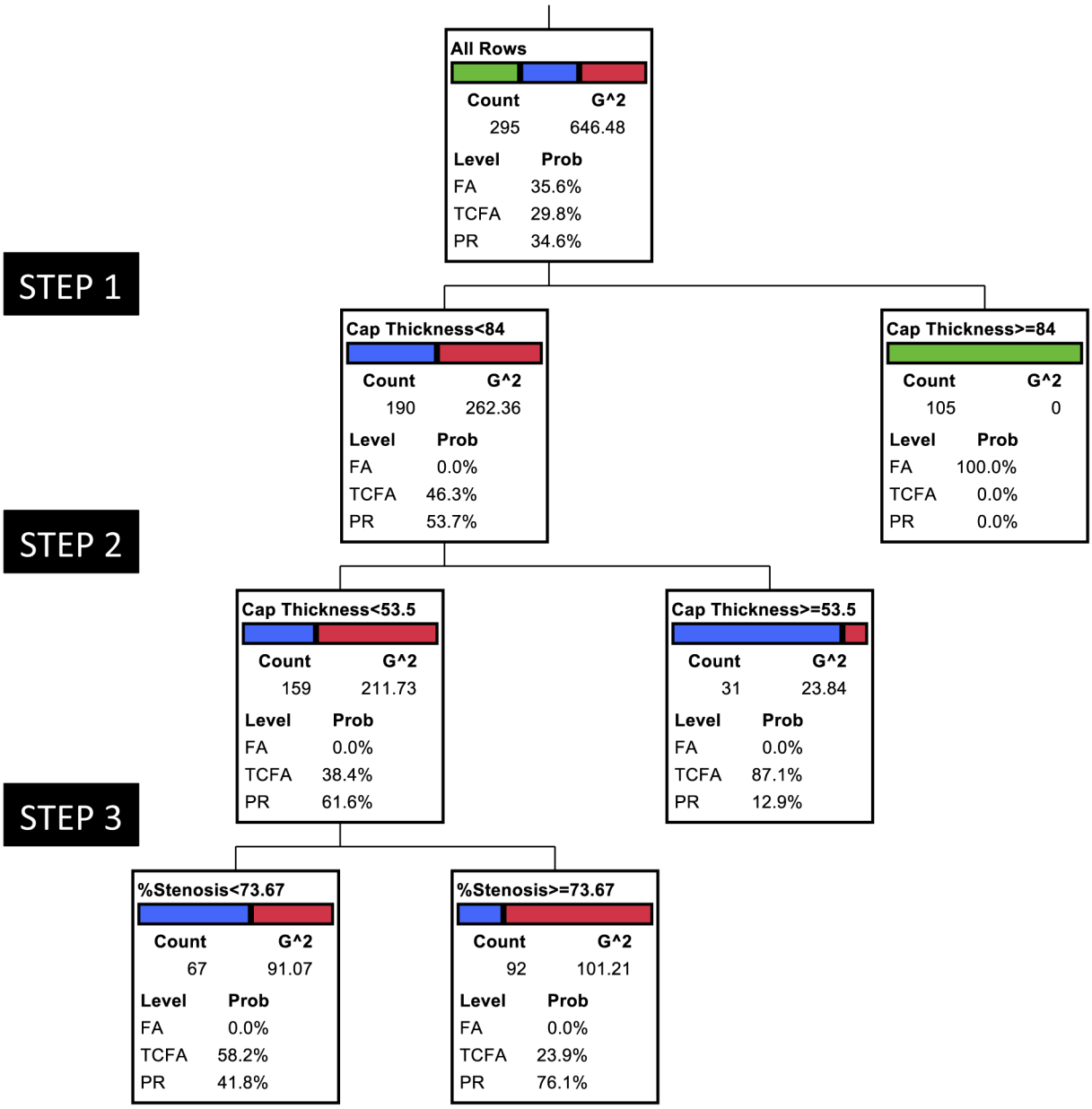

Figure 4. Multivariate RPA Model Including All Cases and All Candidate Variables

Cap thickness was the key plaque characteristic in its ability to discriminate between the 3 plaque types, with all stable FA **(green)** separated into a subgroup of >84 μm. TCAP in PR measured <54 μm **(red). Blue** represents TCFA. The receiver-operating characteristic curve generated from the analysis suggested the following area under the curve: FA, 0.82; TCFA, 0.58; and PR, 0.72. G^2 statistic is a likelihood-ratio chi-square test on which the candidate variables are evaluated for inclusion in the partitioning process. Similar to the Pearson chi-square test (and asymptotically equal), G^2 is a goodness-of-fit test and considered more appropriate for smaller samples and for nested models. RPA = recursive partitioning analysis; other abbreviations as in Figure 1.

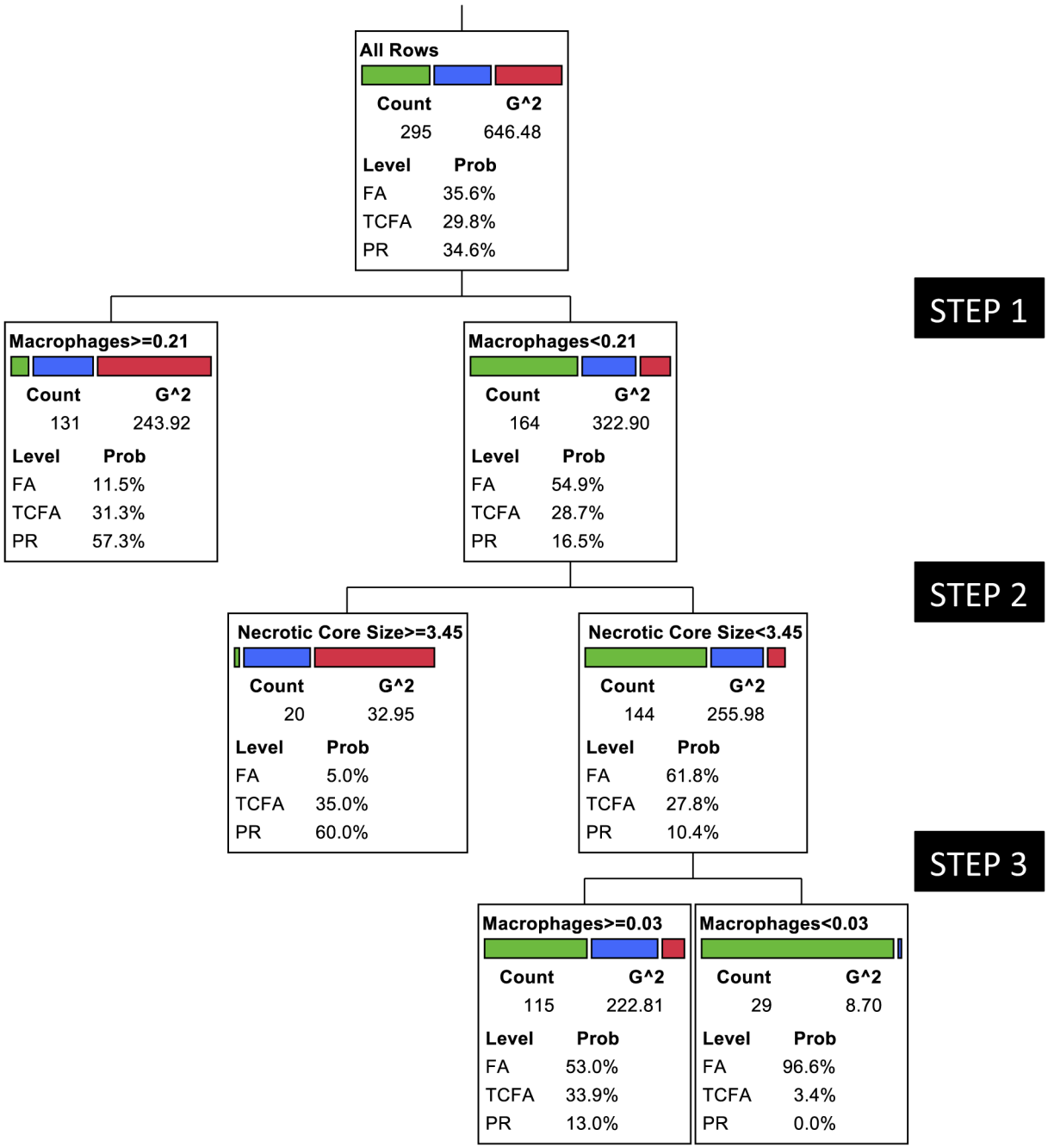

Figure 5. Multivariate RPA Model Including All Cases But Excluding Cap Thickness as the Candidate Variable

Predominance of macrophage infiltration identified a majority of PR **(red)** and TCFA **(blue)**. TCFA and PR in the less-inflamed group (contaminating the FA group) showed larger NC. The few remaining less inflamed and small core PR and TCFA could be isolated from FA **(green)** once again by the degree of inflammation. The receiver-operating characteristic curve generated from the analysis suggested the following area under the curve: FA, 0.82; TCFA, 0.58; and PR, 0.72. Essentially, similar results were observed in re-analysis including only the lesions showing 50% to 75% luminal diameter stenosis; area under the curve: FA, 0.81; TCFA, 0.70; and PR, 0.85. The results were similar for those

with >75% diameter stenosis; area under the curve: FA, 0.86; TCFA, 0.59; and PR, 0.82. Abbreviations as in Figures 1 and 4.

J Am Coll Cardiol. Author manuscript; available in PMC 2014 February 21.

Table 1

Descriptive Statistics for Sample Characteristics

	Total (n = 295)		FA (n = 105)		TCFA (n = 88)		Rupture (n = 102)	
Characteristic	**Mean ± SD**	**Median (range)**	**Mean ± SD**	**Median (range)**	**Mean ± SD**	**Median (range)**	**Mean ± SD**	**Median (range)**
Age (yrs)	55.1 ± 13.5	53 (29–89)	57.8 ± 14.2	55 (34–89)	56.9 ± 14.0	53 (34–89)	50.7 ± 11.2	47 (29–84)
TCAP (cap thickness), mm	0.16 ± 0.21	0.05 (0.01–0.96)	0.4 ± 0.19	0.37 (0.08–0.96)	0.04 ± 0.02	0.03 (0.01–0.06)	0.03 ± 0.01	0.02 (0.01–0.06)
EEL area, mm^2	13.9 ± 5.8	12.73 (4.6–35.0)	11.6 ± 4.5	10.6 (4.6–33.9)	14 ± 5.9	12.7 (5.2–29.7)	16 ± 6.1	14 (4.7–35)
IEL area, mm^2	12.2 ± 5.5	11.16 (3.2–32.4)	10.1 ± 4	9.4 (4.2–28.8)	12.4 ± 5.5	11.3 (4.2–28)	14.2 ± 5.9	13 (3.2–32.4)
Lumen area, mm^2	3.1 ± 2.4	2.43 (0.09–13.7)	2.5 ± 1.8	2.2 (0.1–7.9)	3.6 ± 2.4	2.9 (0.1–11.2)	3.2 ± 2.7	2.3 (0.2–13.7)
Plaque area, mm^2	9.12 ± 4.5	8.23 (2.6–25.5)	7.6 ± 3.3	7.6 (2.6–22.3)	8.8 ± 4.4	7.8 (2.6–23.5)	11 ± 5	9.8 (2.9–25.5)
% Stenosis	75.2 ± 14.5	77.4 (33.0–98.5)	75.8 ± 14.2	76.9 (43.6–97.9)	70.8 ± 14.4	70.6 (34.1–98.5)	78.2 ± 14	82 (33–97.6)
Necrotic core size, mm^2	2.7 ± 3.0	1.74 (0.05–20.5)	1.33 ± 1.0	0.96 (0.05–4.63)	2.26 ± 1.98	1.63 (0.16–9.9)	4.37 ± 4.09	3.08 (0.13–20.46)
% Necrotic core	26.2 ± 8.0	22.0 (1.3–84.8)	17.7 ± 11.5	16.3 (1.3–57.9)	25.2 ± 15.7	22.1 (4.4–63.7)	35.9 ± 20.6	32.5 (1.4–84.8)
Macrophages, mm^2	0.32 ± 0.38	0.17 (0–2.75)	0.12 ± 0.16	0.07 (0–0.86)	0.31 ± 0.36	0.19 (0.01–2.19)	0.53 ± 0.44	0.41 (0.02–2.75)
% Macrophages	3.8 ± 4.5	2.1 (0.03–27.4)	1.8 ± 2.4	0.9 (0–14.5)	4.1 ± 4.5	2.7 (0.2–23.6)	5.7 ± 5.3	4.1 (0.3–27.4)
Total calcification, mm^2	0.51 ± 0.91	0.035 (0–4.9)	0.46 ± 0.81	0.014 (0–3.72)	0.50 ± 0.94	0.048 (0–4.91)	0.575 ± 0.993	0.053 (0–4.94)
% Calcification	5.5 ± 11.2	0.42 (0–79.0)	6.5 ± 13.5	0.19 (0–79.0)	5.3 ± 11.43	0.67 (0–75.6)	4.77 ± 7.67	0.54 (0–35.43)

Values are for 295 specimens, 250 male, and 45 female. Preliminary evaluations indicated skewness for plaque feature distributions, with all tests for normality rejected at $p < 0.001$. Kruskal-Wallis tests showed statistically significant differences by plaque type at $p < 0.01$ for all features with the notable exception of both total and percent calcification. Trend test indicated statistically significant trends in the levels of each feature ($p < 0.001$) with the exception of lumen, percent stenosis, and both measures of calcification.

EEL = external elastic lamina; FA = fibroatheroma; IEL = internal elastic lamina; TCAP = fibrous cap thickness; TCFA = thin-cap fibroatheroma.

Table 2

Recursive Partitioning Models Results

			R^2		ROC, AUC		
Model	**Split Sequence**	**% Contribution to Total Chi-Square**	**Overall**	**5-Fold Cross-Validation**	**FA (n = 105)**	**TCFA (n = 88)**	**RP (n = 102)**
All cases (n = 295) including TCAP	Cap thickness	93.6	0.678	0.665	1.00	0.888	0.897
	% Stenosis	4.4					
All cases (n = 295) excluding TCAP	Macrophages	75.4	0.214	0.197	0.82	0.576	0.774
	Necrotic core	24.6					
50%–75% stenosis, excluding TCAP (n = 113)	Macrophages	86.7	0.249	0.202	0.813	0.698	0.848
	Necrotic core	13.3					
>75% stenosis, excluding TCAP (n = 163)	Macrophages	56.7	0.26	0.206	0.864	0.585	0.817
	Necrotic core	35.5					
	Macrophages	7.8					

Contribution of major discriminators to total chi-square and calculation of area under the curve (AUC) for the diagnostic accuracy.

ROC = receiver-operating characteristic; other abbreviations as in Table 1.